Dalton Transactions

Supporting Information

Novel organically linked Zn^{II} hydrogenselenite coordination polymers: synthesis, characterization, and efficient TiO_2 photosensitization for enhanced photocatalytic hydrogen production

Andressa Lunardi,[a] Tanize Bortolotto, [a] Camila Nunes Cechin,[a] Natália de Freitas Daudt,[b] Melina de Azevedo Mello,[c] Sailer S. dos Santos,[a] Roberta Cargnelutti,[a] Ernesto Schulz Lang[a] and Bárbara Tirloni*[a]

[a.] *Departamento de Química, Universidade Federal de Santa Maria – UFSM, Laboratório de Materiais Inorgânicos – LMI, 97105-900, Santa Maria, RS, Brazil.*
E-mail: barbara.tirloni@ufsm.br

[b.] *Departamento de Engenharia Mecânica, Universidade Federal de Santa Maria – UFSM, 97105-900, Santa Maria, RS, Brazil.*

[c.] *Colégio Técnico Industrial de Santa Maria - CTISM – Universidade Federal de Santa Maria – UFSM, 97105-900, Santa Maria, RS, Brazil.*

Table of Contents

Table S1. Crystallographic and structure refinement data for compounds **1**-**2**.

	1	**2**
Formula	$C_{10}H_{10}N_2O_6Se_2Zn$	$C_{12}H_{10}N_2O_6Se_2Zn$
F.W. ($g.mol^{-1}$)	477.49	501.51
Crystal system	Monoclinic	Triclinic
Space group	C2/*c*	P-*1*
a (Å)	16.9676(8)	7.4196(6)
b (Å)	10.9596(5)	9.7542(9)
c (Å)	7.4548(3)	11.1087(10)
α (°)	90	71.238(3)
β (°)	95.478(2)	88.646(3)
γ (°)	90	87.737(3)
T (K)	299(2)	299(2)
V ($Å^3$)	1379.95(11)	760.60(12)
Z	4	1
$\rho_{calc.}$ ($g.cm^{-3}$)	2.289	2.181
μ (mm^{-1})	7.083	6.431
F(000)	912	480
Refl. collected	28932	23456
Refl. unique *(R_{int})*	2132 [0.0835]	4648 [0.0673]
R_1 *[I > 2σ(I)]*	R_1 = 0.0418	R_1 = 0.0561
wR_2 [I > 2σ(I)]	wR_2 = 0.0711	wR_2 = 0.1405
R_1 (all data)[a]	R_1 = 0.0778	R_1 = 0.1025
wR_2 (all data)[b]	wR_2 = 0.0799	wR_2 = 0.1558
Goodness-of-fit on F^2	1.046	1.093
Largest diff. peak and hole ($e.Å^{-3}$)	0.687 and -0.575	1.336 and -0.730

[a]$R_1 = |F_o - F_c|/|F_o|$; [b]$wR_2 = [w(F_o^2 - F_c^2)^2/(wF_o^2)]^{-1/2}$.

Table S2. Selected bond lengths (Å) and angles (°) for compounds **1**-**2**.

Bond lengths (Å)		**Bond angles (°)**	
1			
Zn1–N1	2.201(3)	N1–Zn1–N1’	74.71(15)
Zn1–O1	2.072(2)	N1’–Zn1–O2’’	91.34(10)
Zn1–O2’’	2.098(2)	N1’–Zn1–O1	88.44(10)
Se1–O1	1.654(2)	O2’’–Zn1–O1	88.90(10)
Se1–O2	1.668(2)	O2–Se1–O1	107.49(12)
Se1–O3	1.754(3)	O2–Se1–O3	99.79(13)
O3–H3A	0.820(3)	O1–Se1–O3	100.44(13)
2			
Zn1–N1	2.203(6)	N1–Zn1–N2	74.9(2)
Zn1–N2	2.219(5)	N1–Zn1–O5’	88.4(2)
Zn1–O1	2.070(5)	O4–Zn1–O1	109.62(19)
Zn1–O4	2.064(5)	O4–Zn1–O5’	90.12(19)
Zn1–O5’	2.090(5)	O4–Zn1–N2	87.3(2)
Se1–O1	1.657(5)	O2–Se1–O1	100.3(2)
Se1–O2	1.756(5)	O2–Se1–O3	99.3(2)
Se1–O3	1.668(5)	O1–Se1–O3	106.7(2)
O2–H2A	0.820(5)		

1 (’): -*x*+1,*y*,-*z*+1/2; (‘’): -*x*+1,-*y*+1,-*z*+1

2 (’): -*x*+2,-*y*+1,-*z*+1

Table S3. Selected hydrogen bond lengths (Å) and angles (°) for compounds **1**-**2**.

D-H···A	d(D-H)	d(H···A)	d(D···A)	<(DHA)
1				
O3–H3A···O2’	0.82	1.87	2.685(4)	172.3
2				
O2–H2A···O5	0.82	1.90	2.699(7)	164.1

1 (’): -*x*+1,*y*,-*z*+1/2

Table S4. Time (t) and temperature (T) used to obtain **1**-**2**.

n	t_n (minutes)[a]	T_n (°C)[b]
0	–	90
1	60	110
2	60	130
3	60	140
4	240	140
5	120	130
6	120	120
7	120	100
8	120	80
9	300	40
Total time: 20 h, with 4 h at 140 °C.		

a) time required for the oven to reach T_n; b) temperature in the reactor.

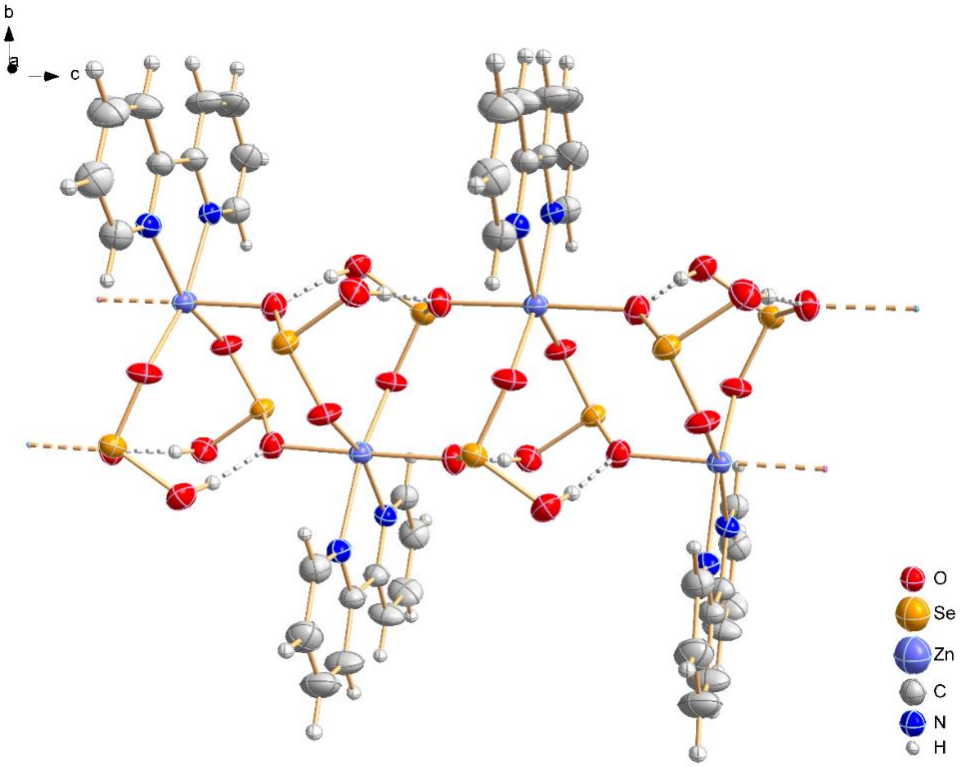

Figure S1. ORTEP[12] representation of the polymeric structure of $[Zn(\mu\text{-}HSeO_3)_2(bipy)]_n$ (**1**). The thermal ellipsoids indicate the 50% probability level.

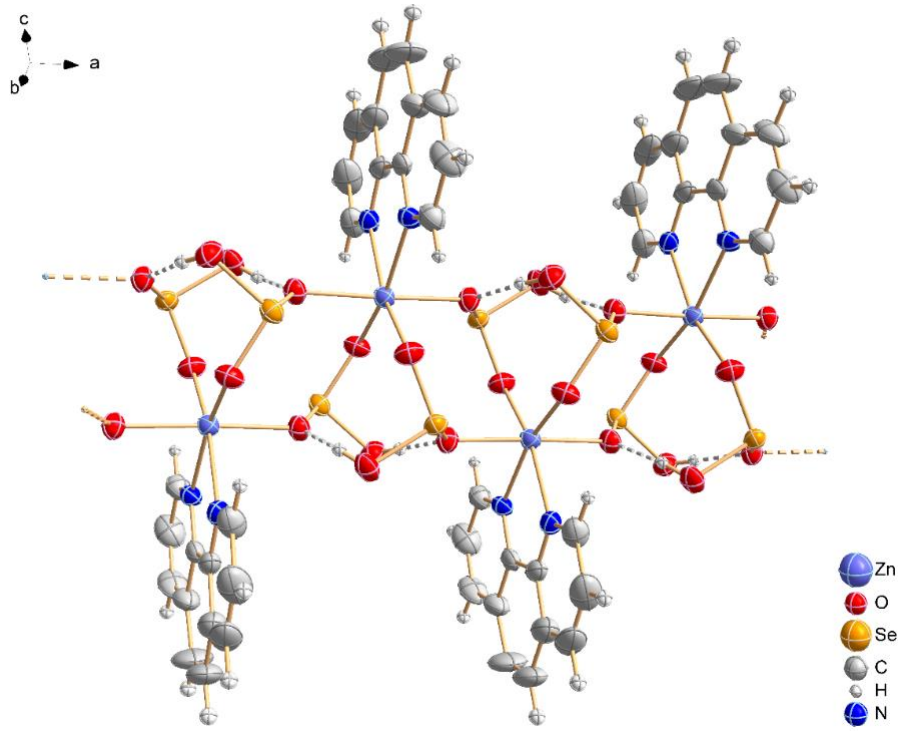

Figure S2. ORTEP[12] representation of the polymeric structure of $[Zn(\mu\text{-}HSeO_3)_2(phen)]_n$ (**2**). The thermal ellipsoids indicate the 50% probability level.

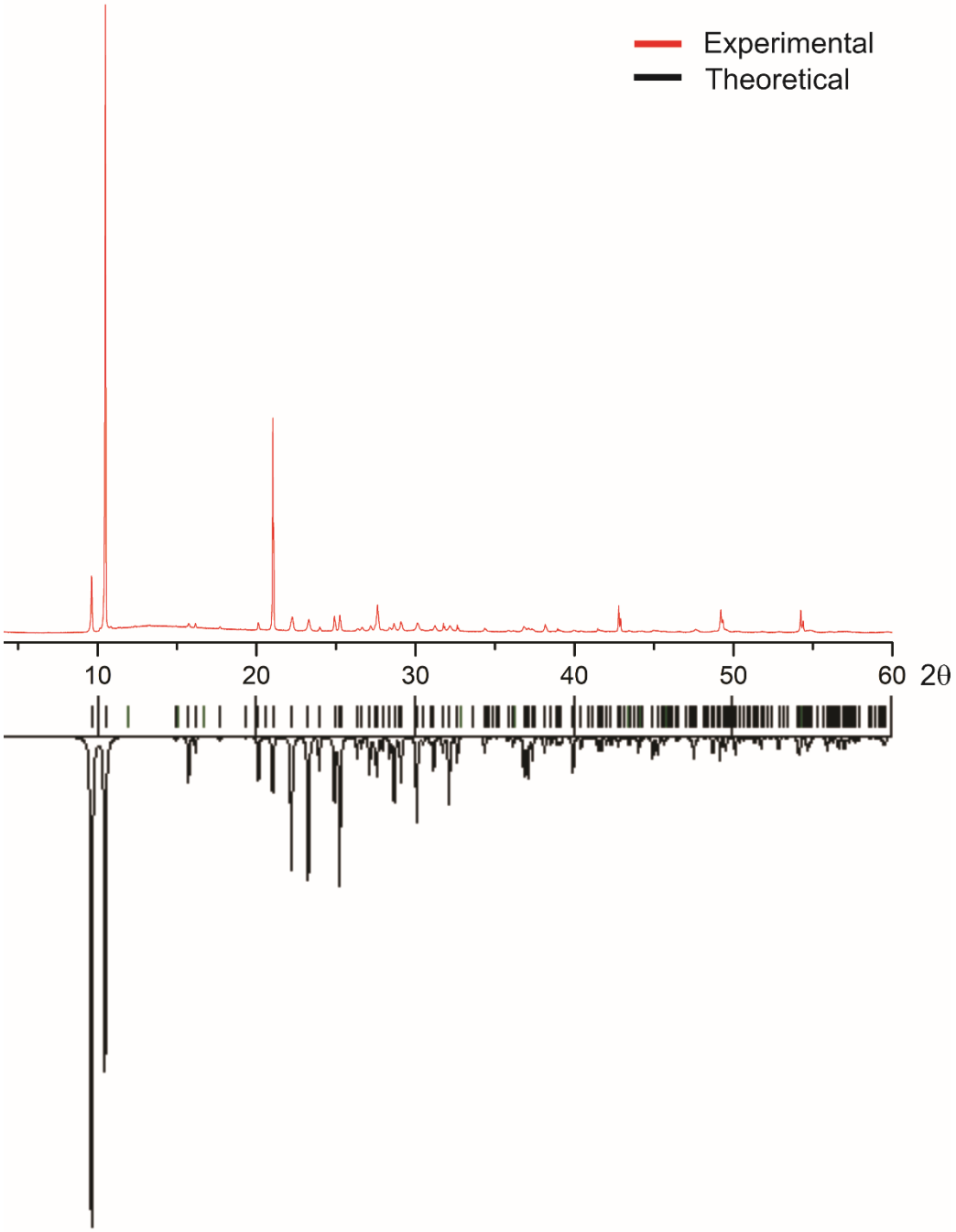

Figure S3. Simulated and experimental PXRD pattern for $[Zn(\mu\text{-}HSeO_3)_2(bipy)]_n$ (**1**).

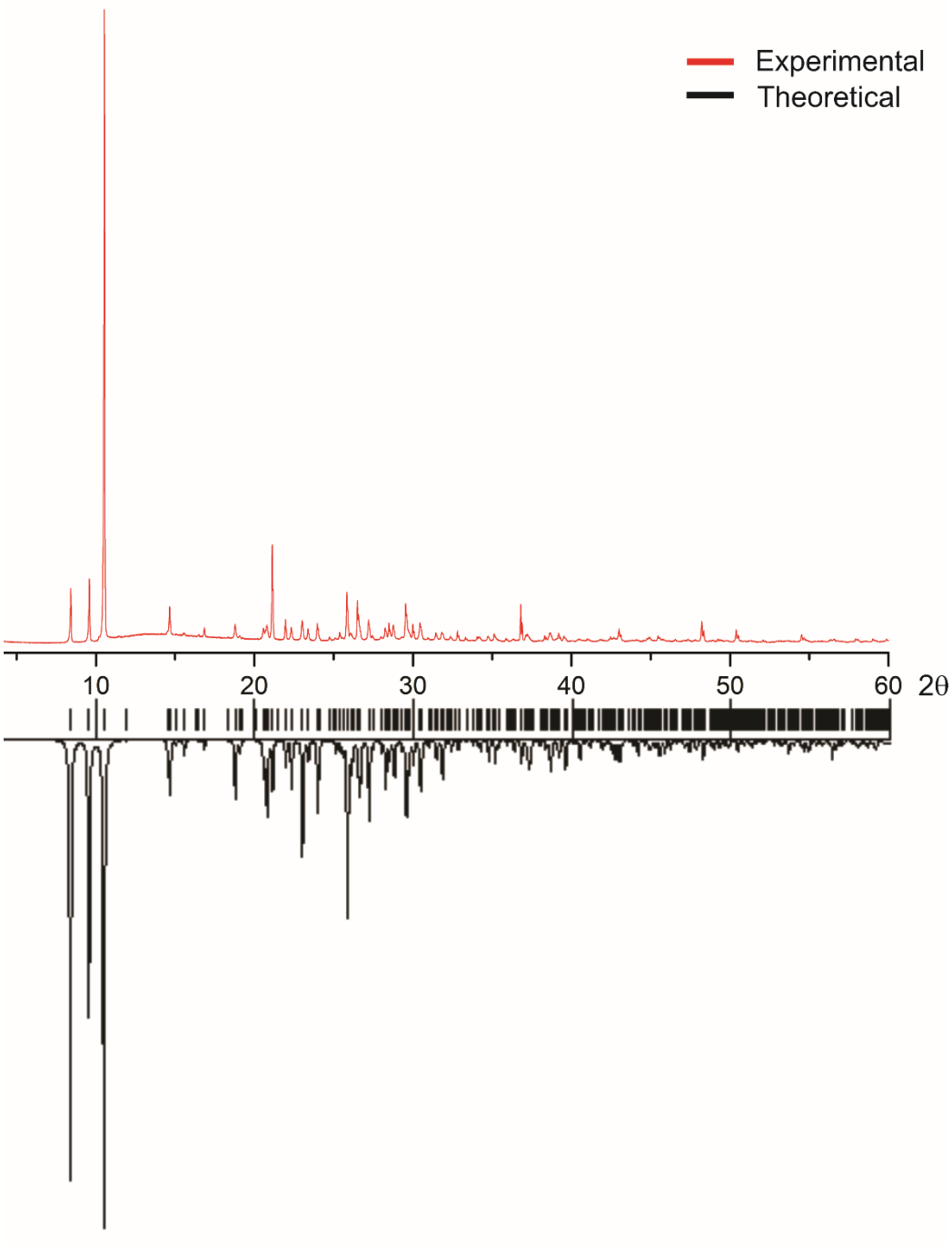

Figure S4. Simulated and experimental PXRD pattern for $[Zn(\mu\text{-}HSeO_3)_2(phen)]_n$ (**2**).

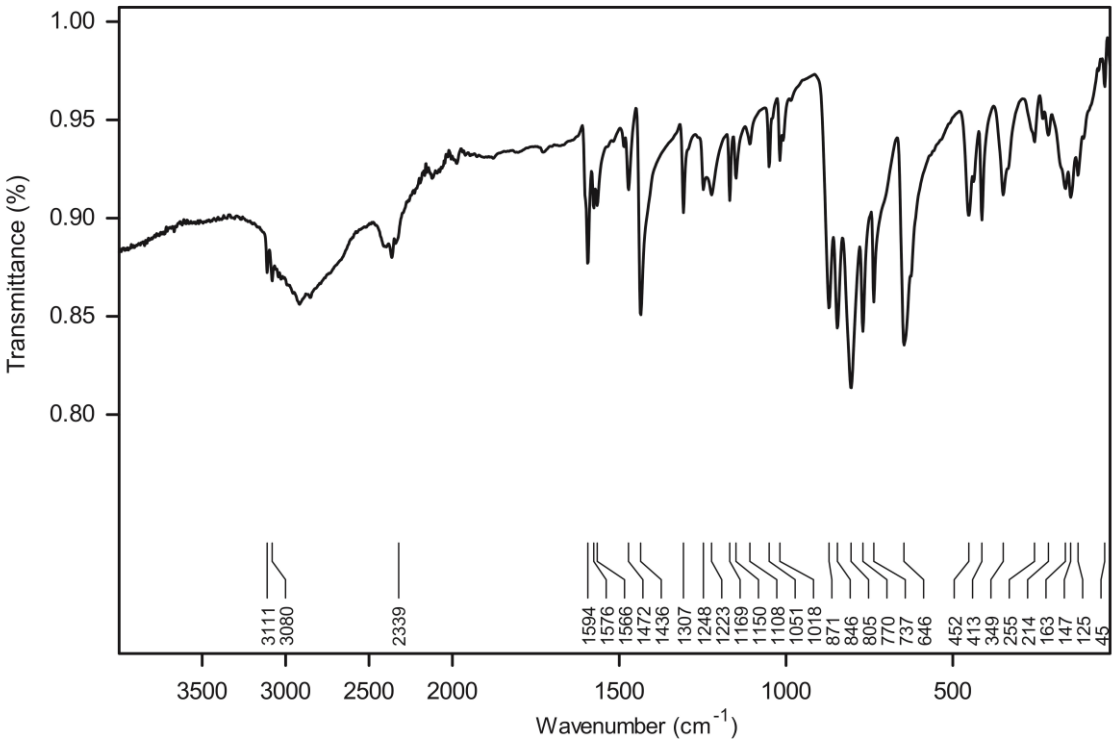

Figure S5. FT-IR spectrum for $[Zn(\mu\text{-}HSeO_3)_2(bipy)]_n$ (**1**).

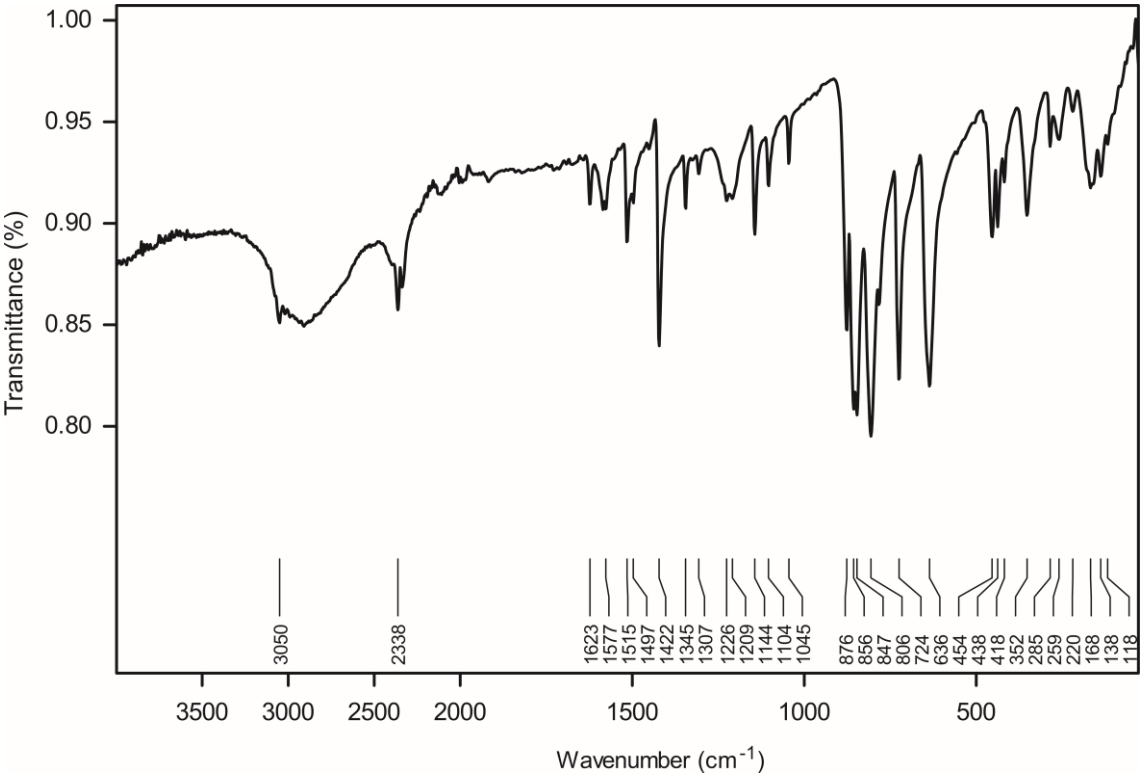

Figure S6. FT-IR spectrum for $[Zn(\mu\text{-}HSeO_3)_2(phen)]_n$ (**2**).

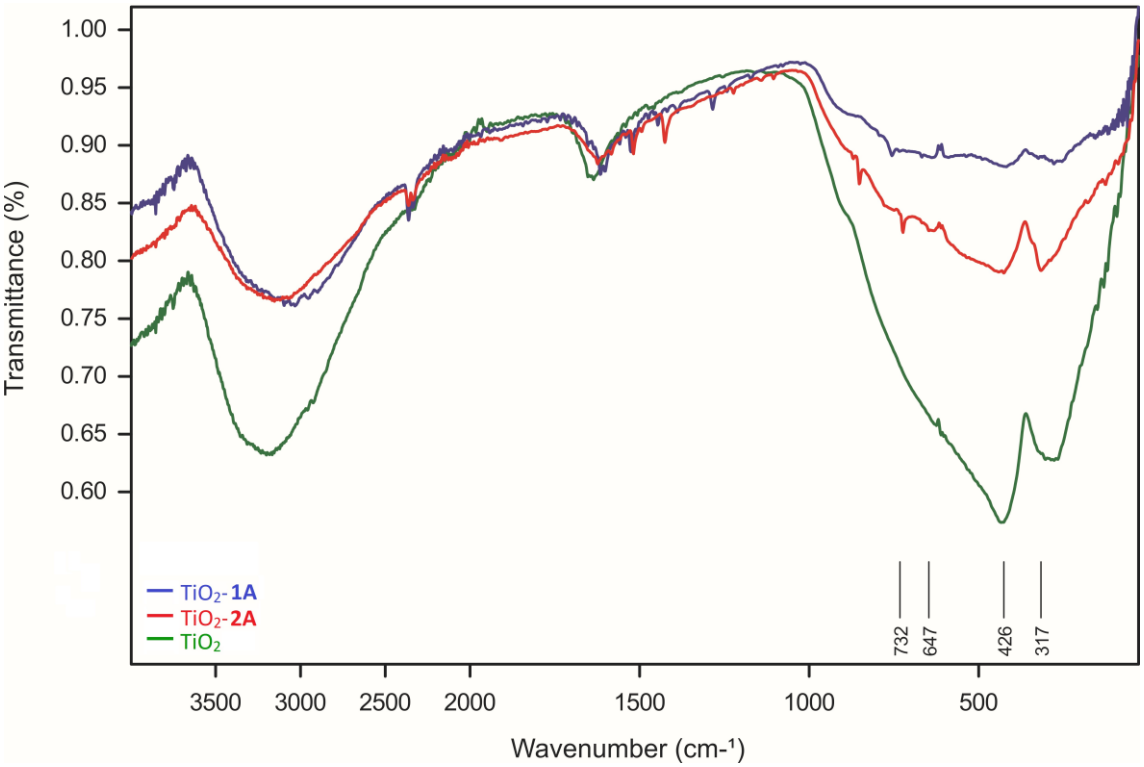

Figure S7. FT-IR spectrum of photocatalysts TiO_2-**1A,** TiO_2-**2A** and TiO_2.

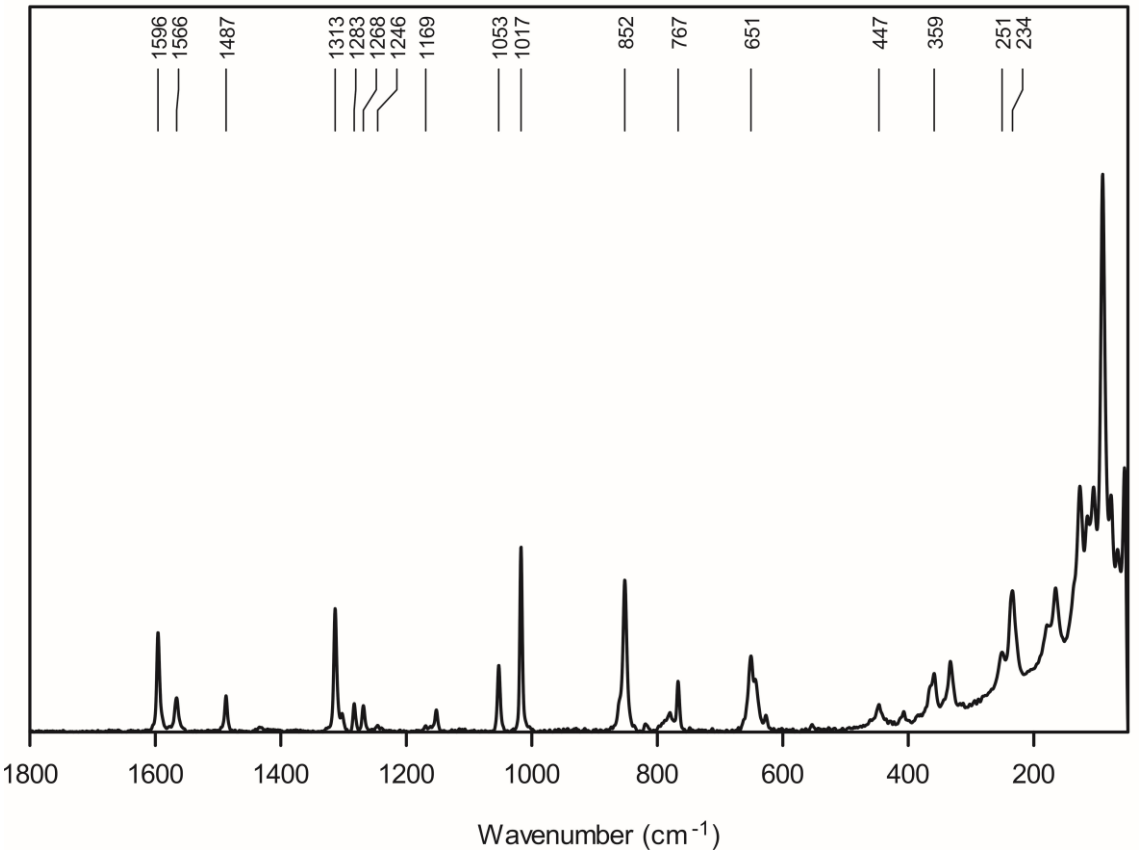

Figure S8. Confocal Raman spectrum for $[Zn(\mu\text{-}HSeO_3)_2(bipy)]_n$ (**1**).

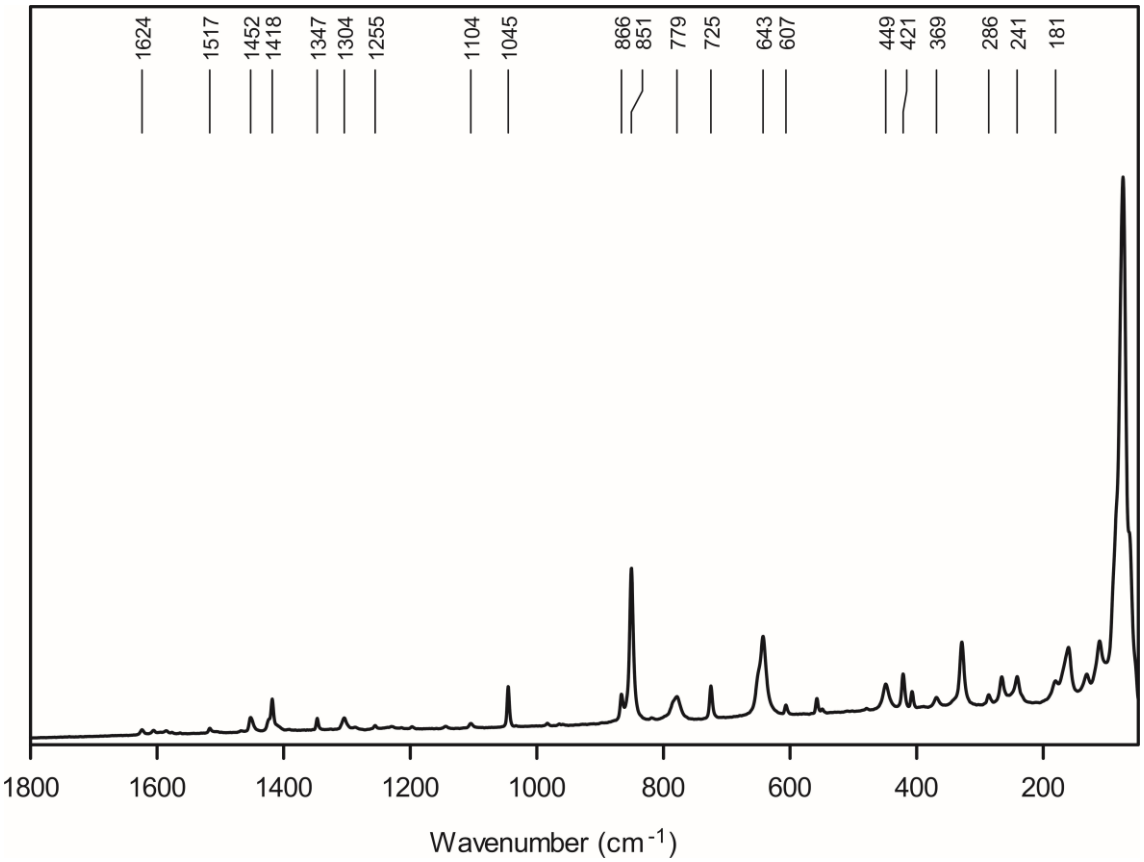

Figure S9. Confocal Raman spectrum for $[Zn(\mu\text{-}HSeO_3)_2(phen)]_n$ (**2**).

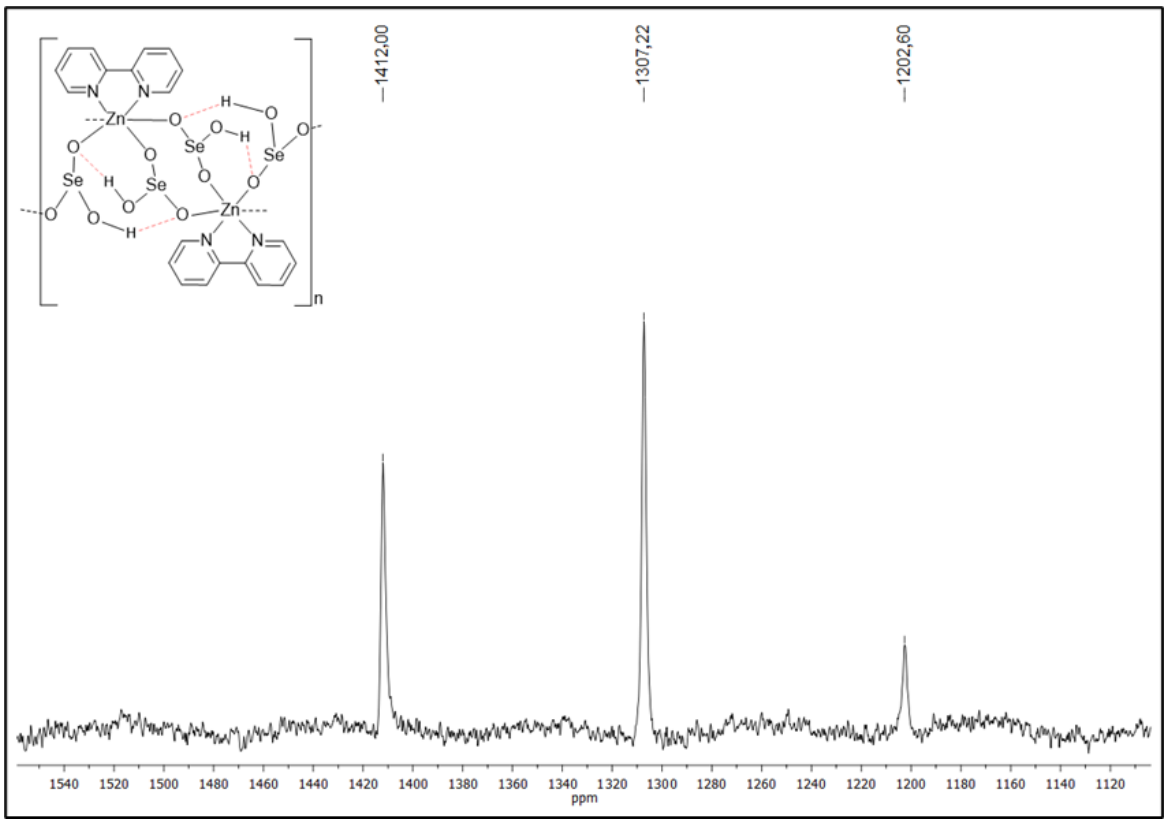

Figure S10. ^{77}Se NMR spectrum for $[Zn(\mu\text{-}HSeO_3)_2(bipy)]_n$ (**1**)

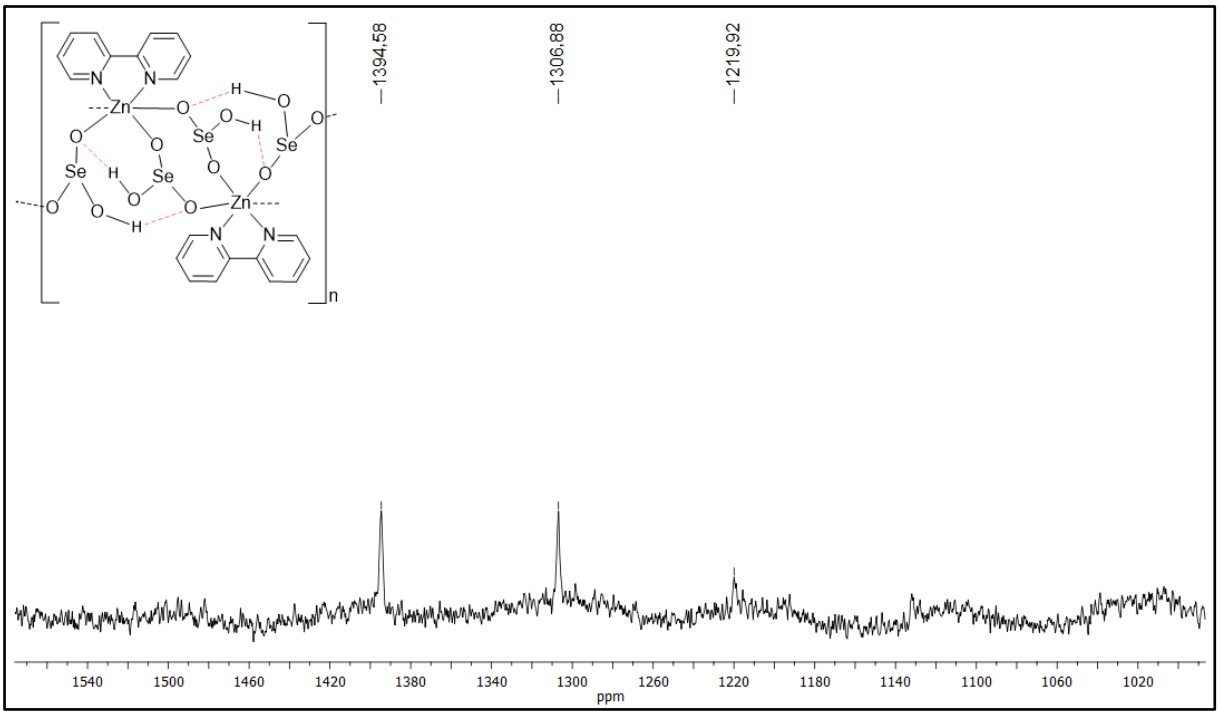

Figure S11. ^{77}Se NMR spectrum for $[Zn(\mu\text{-}HSeO_3)_2(bipy)]_n$ (**1**) using 10 kHz rotation.

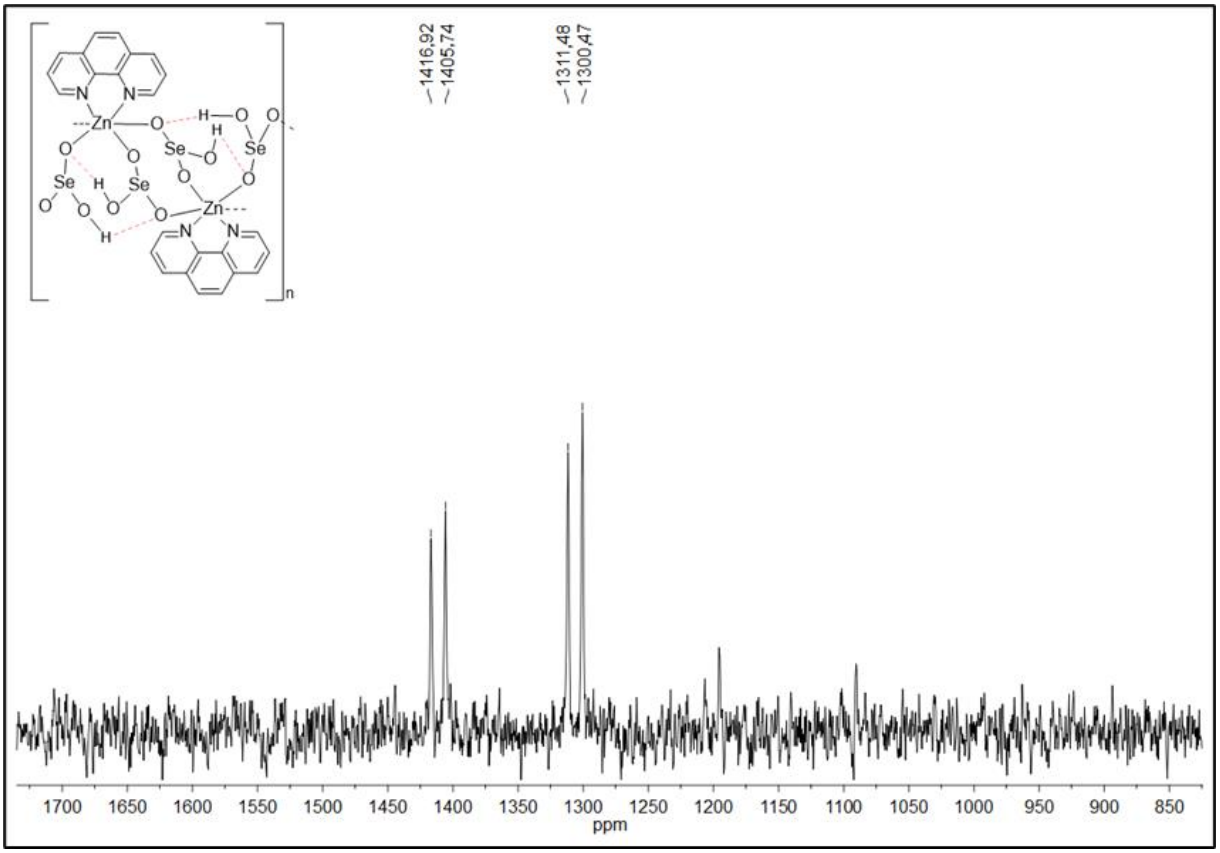

Figure S12. ^{77}Se NMR spectrum for $[Zn(\mu\text{-}HSeO_3)_2(phen)]_n$ (**2**).

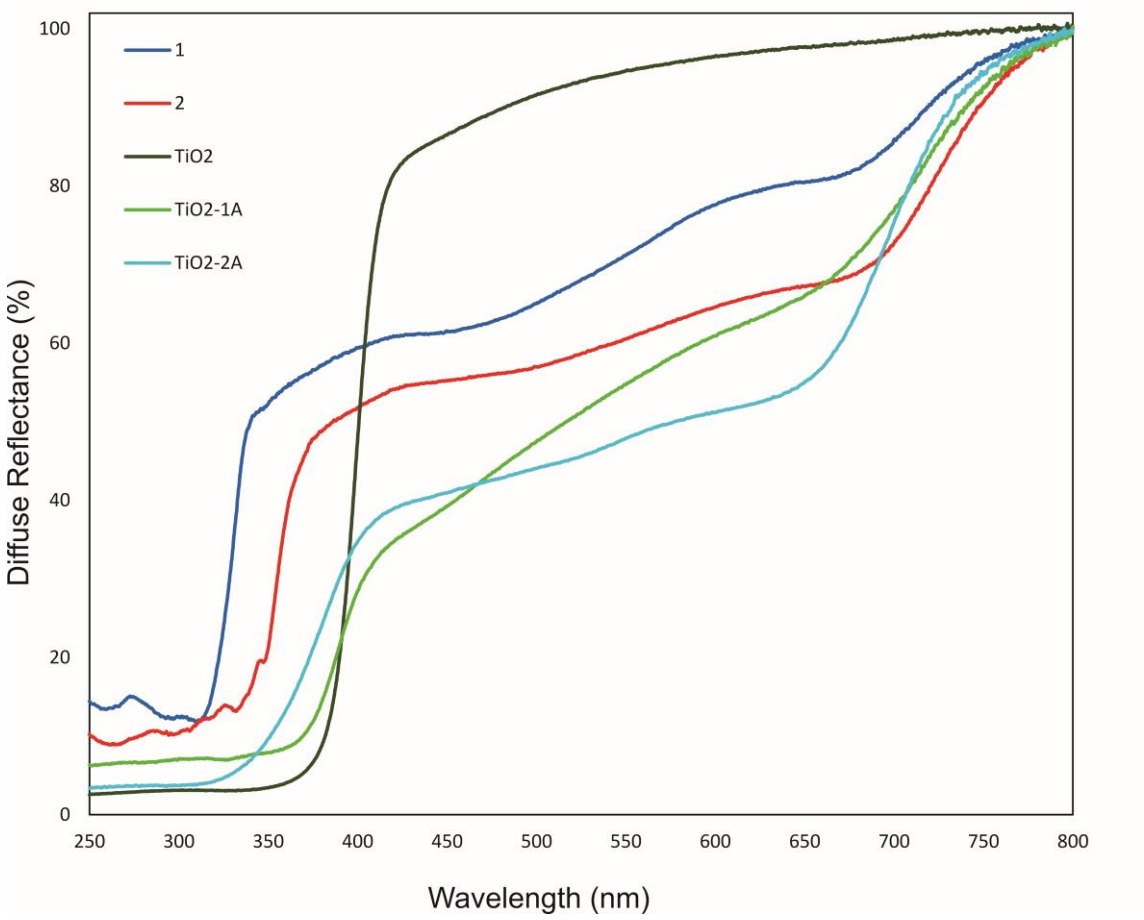

Figure S13. Diffuse reflectance spectra of **1**-**2**, TiO_2, TiO_2-**1A** and TiO_2-**2A**.

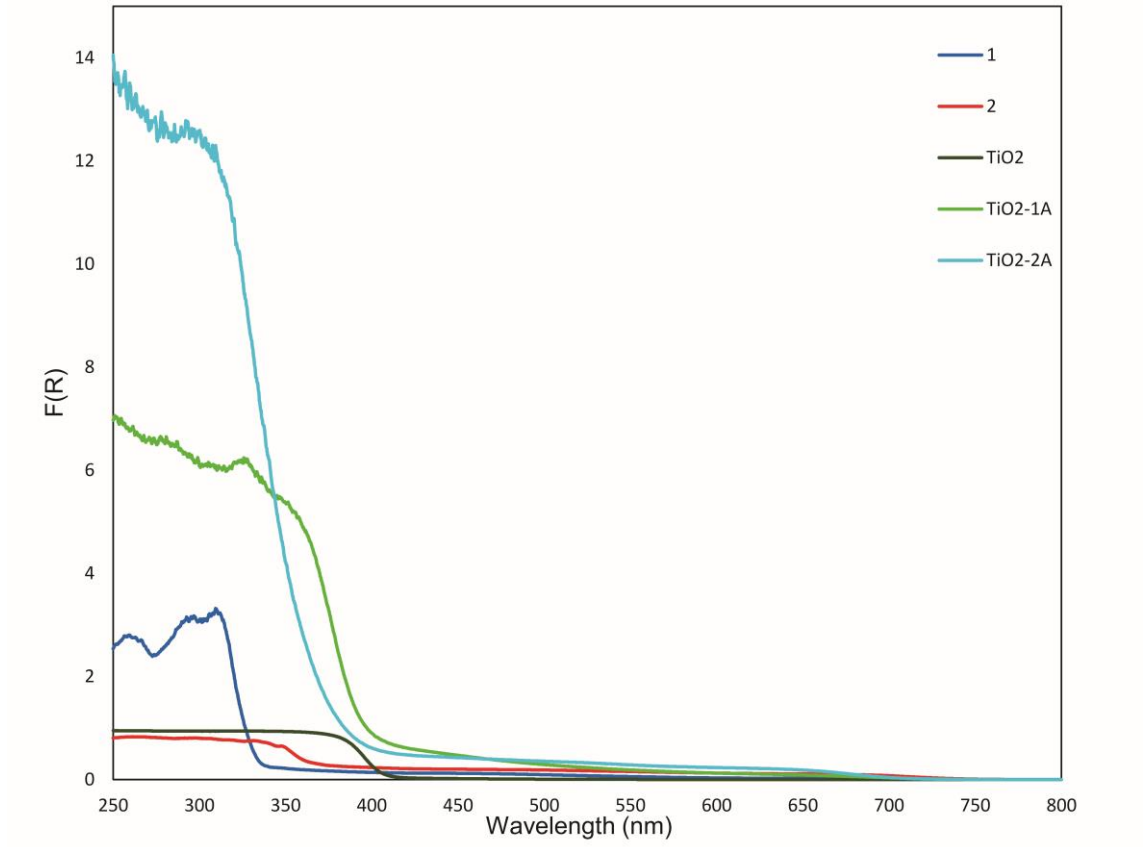

Figure S14. Kubelka-Munk absorbance spectra of **1**-**2**, TiO_2, TiO_2-**1A** and TiO_2-**2A**.

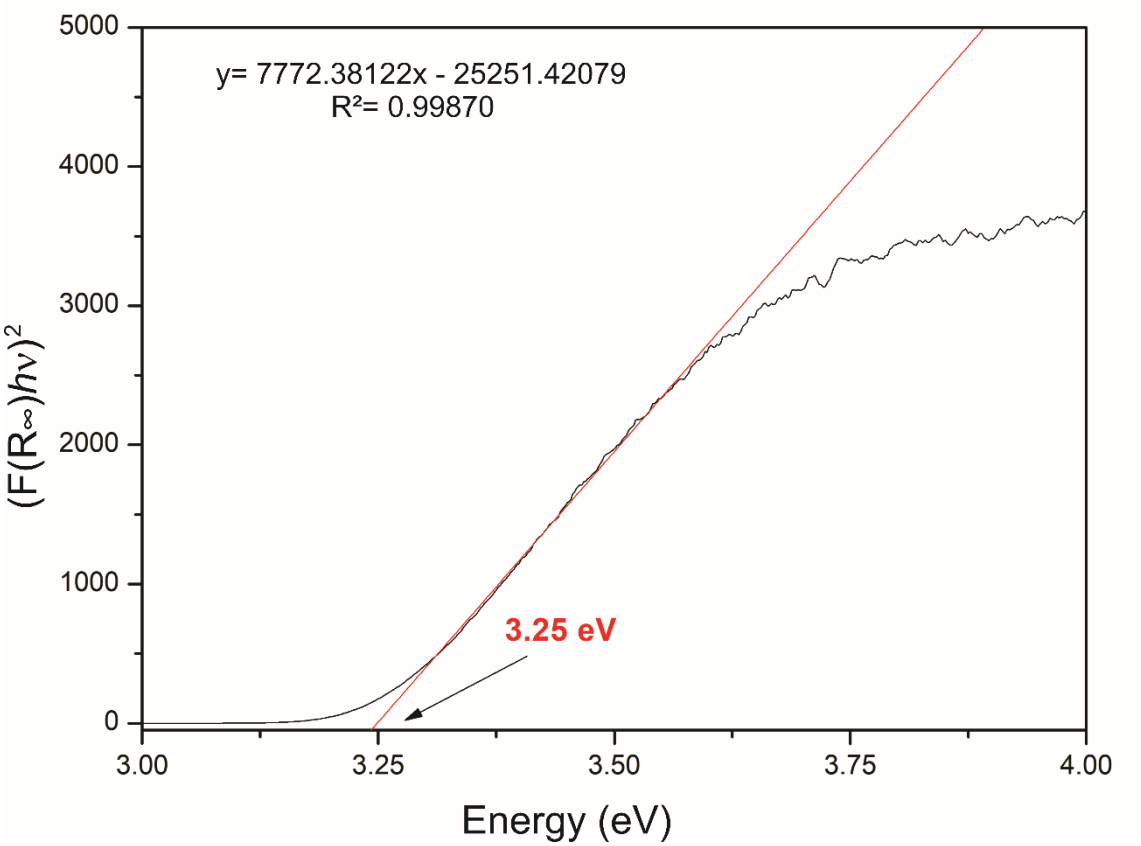

Figure S15. Graphical determination of the E_g value of TiO_2.

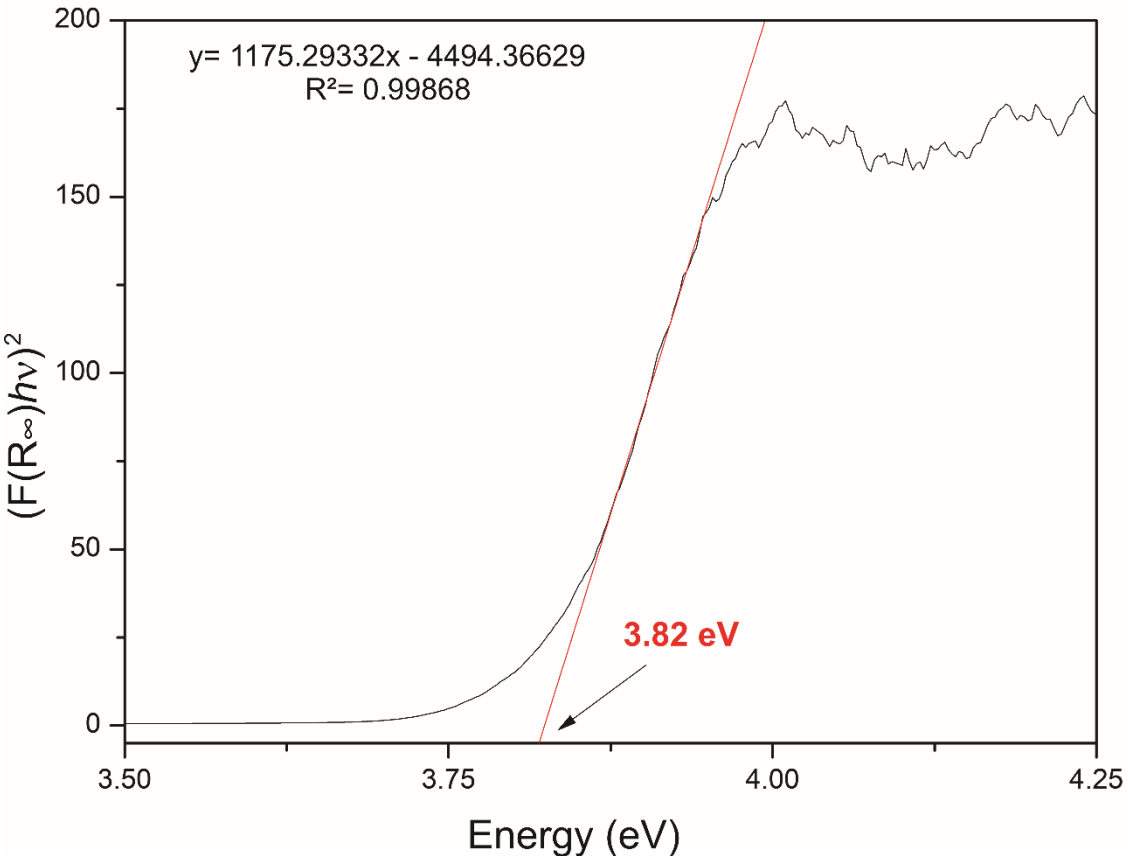

Figure S16. Graphical determination of the E_g value of $[Zn(\mu\text{-}HSeO_3)_2(bipy)]_n$ (**1**).

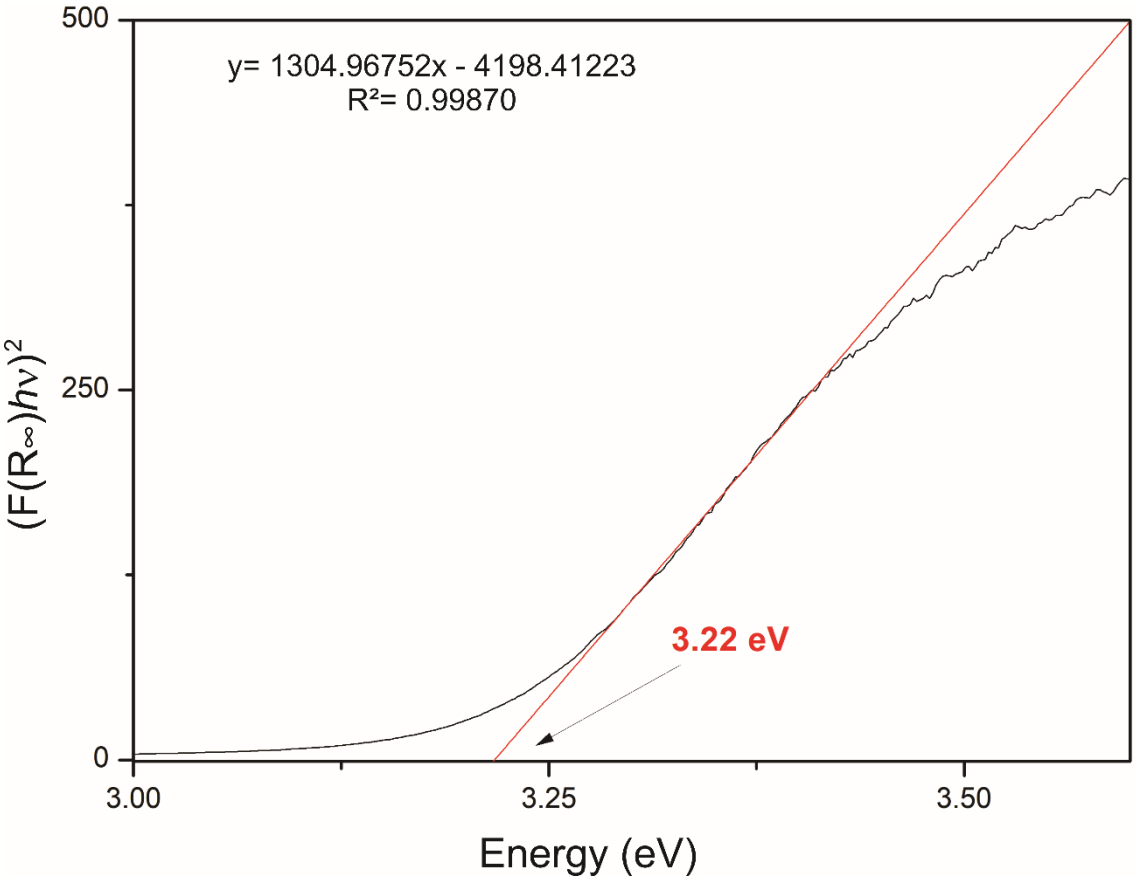

Figure S17. Graphical determination of the E_g value of TiO_2-**1A**.

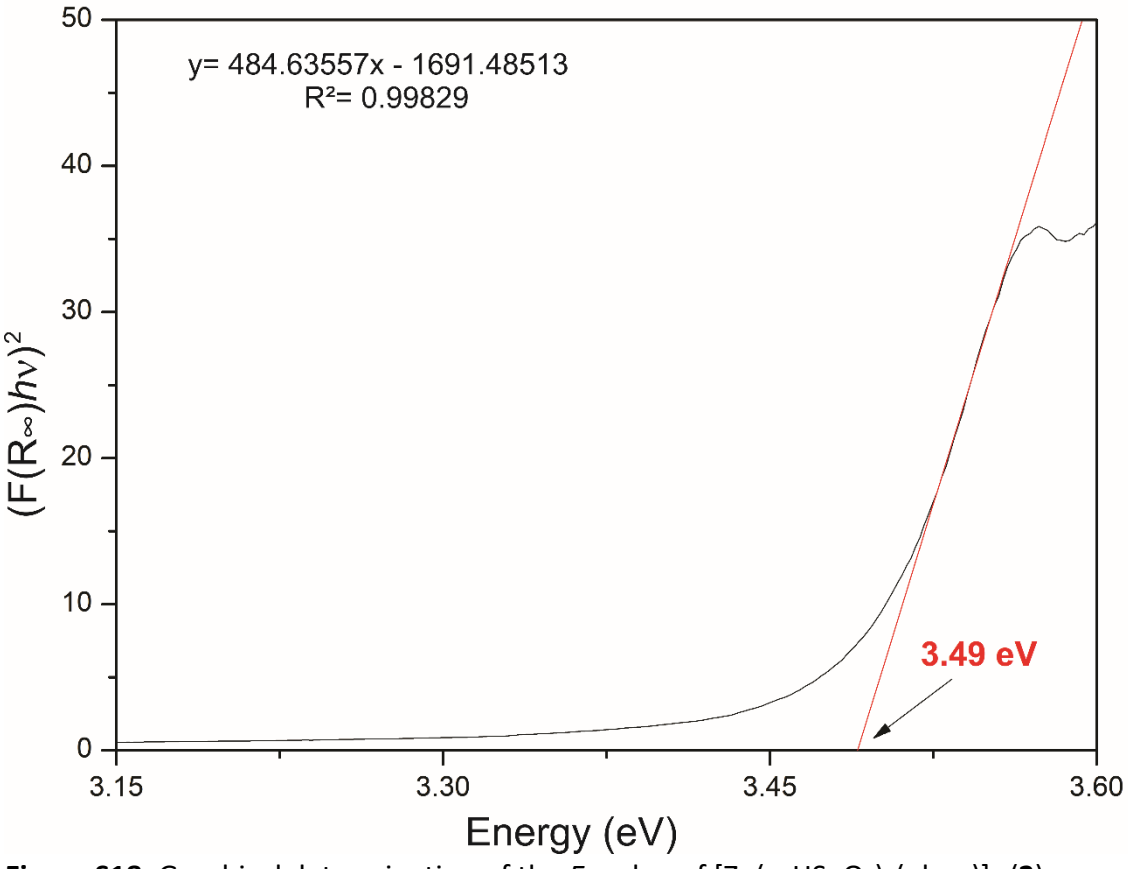

Figure S18. Graphical determination of the E_g value of $[Zn(\mu\text{-}HSeO_3)_2(phen)]_n$ (**2**).

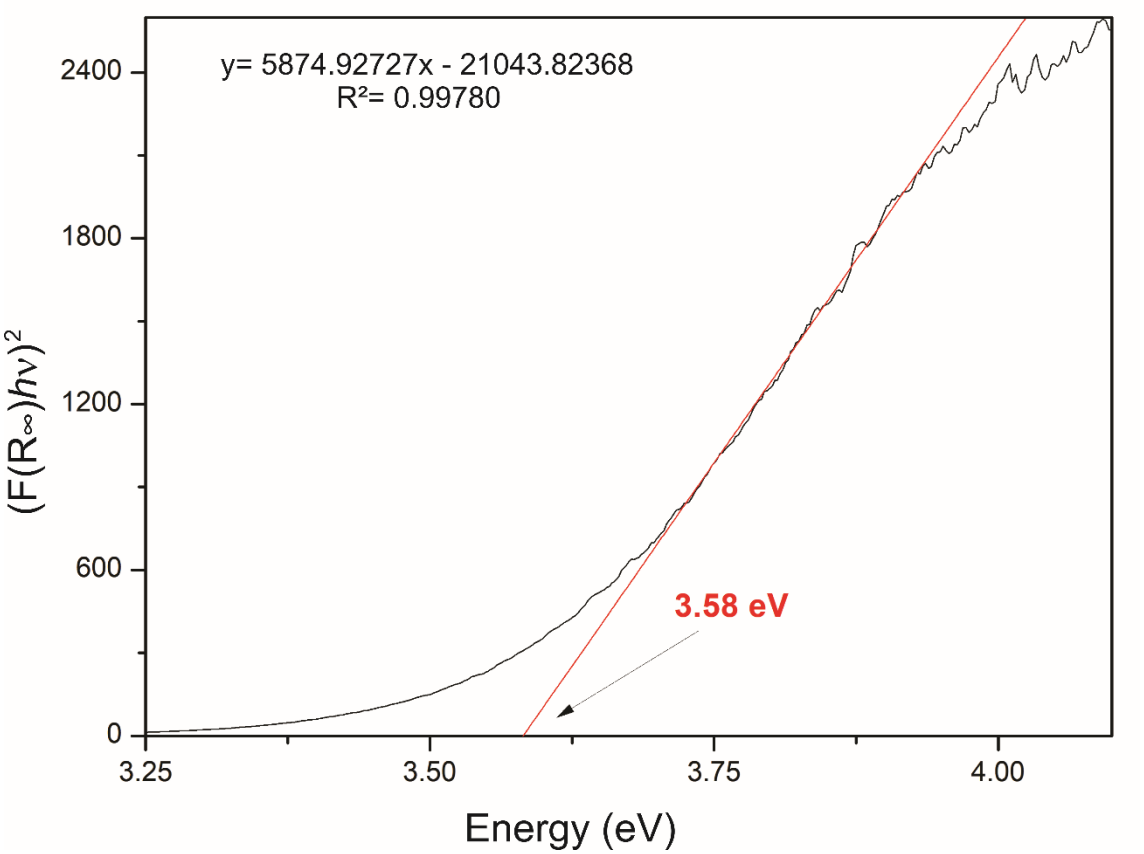

Figure S19. Graphical determination of the E_g value of TiO_2-**2A**.

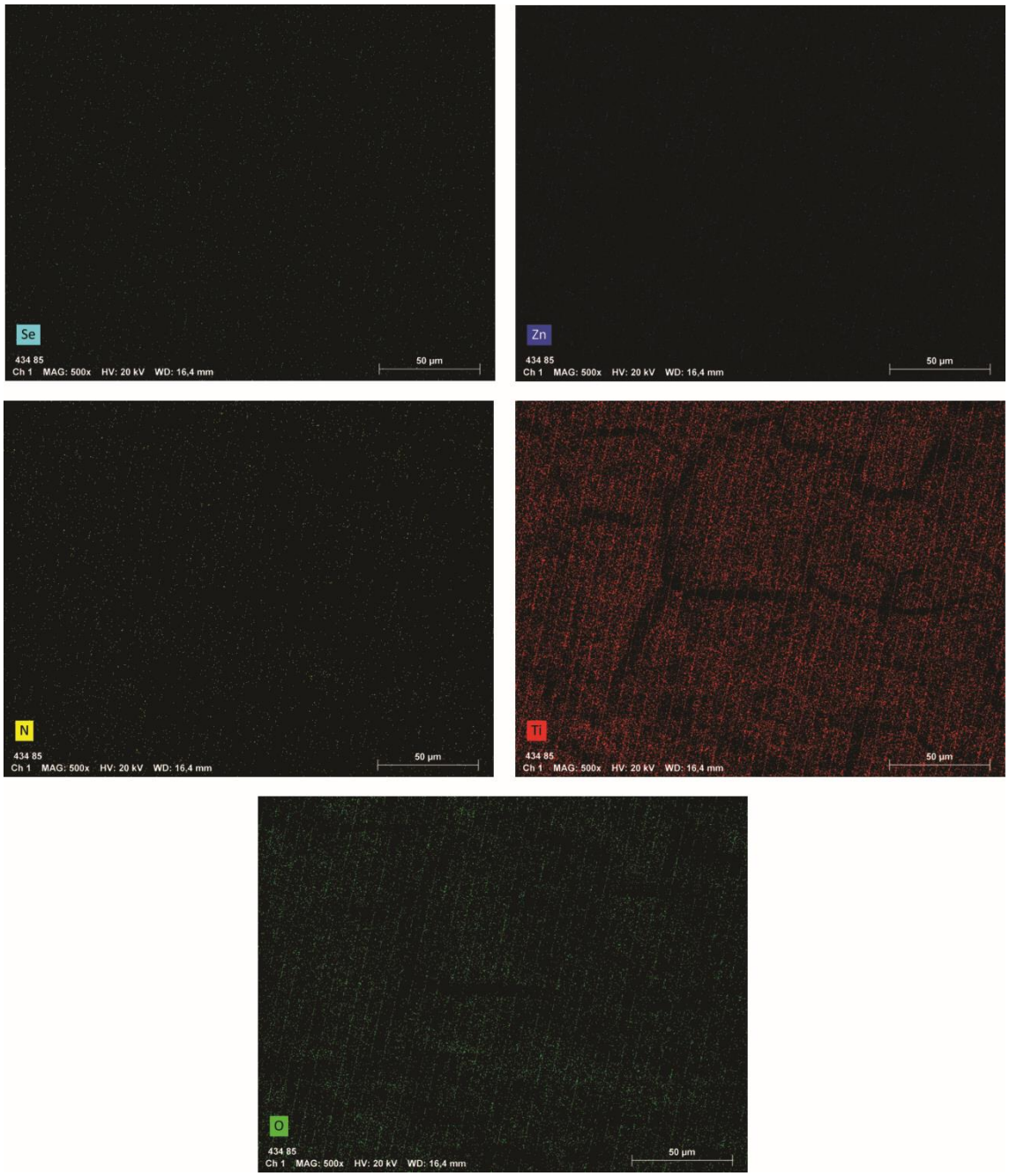

Figure S20. Element mapping for photocatalyst TiO_2-**1A**.

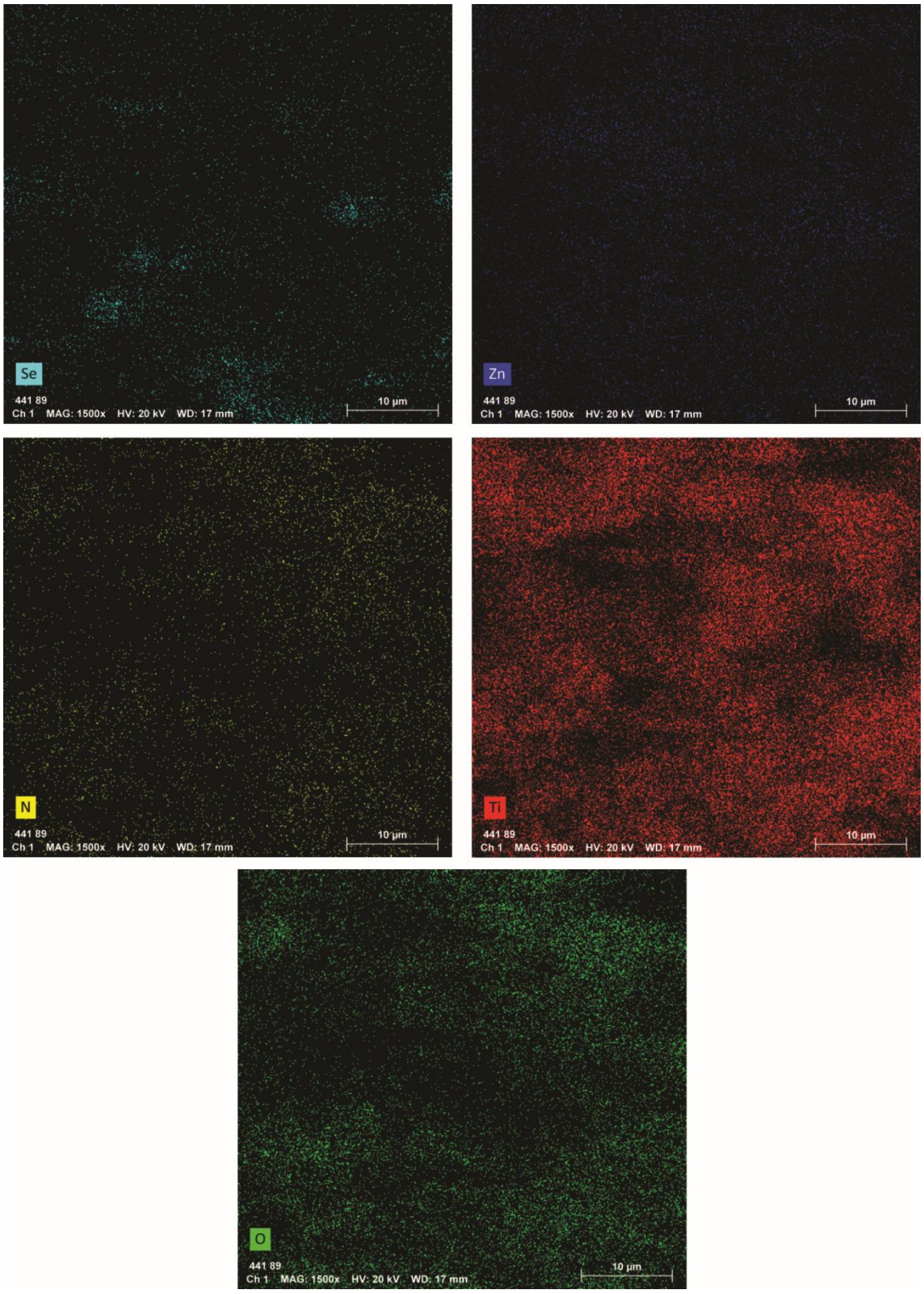

Figure S21. Element mapping for photocatalyst TiO_2-**2A**.

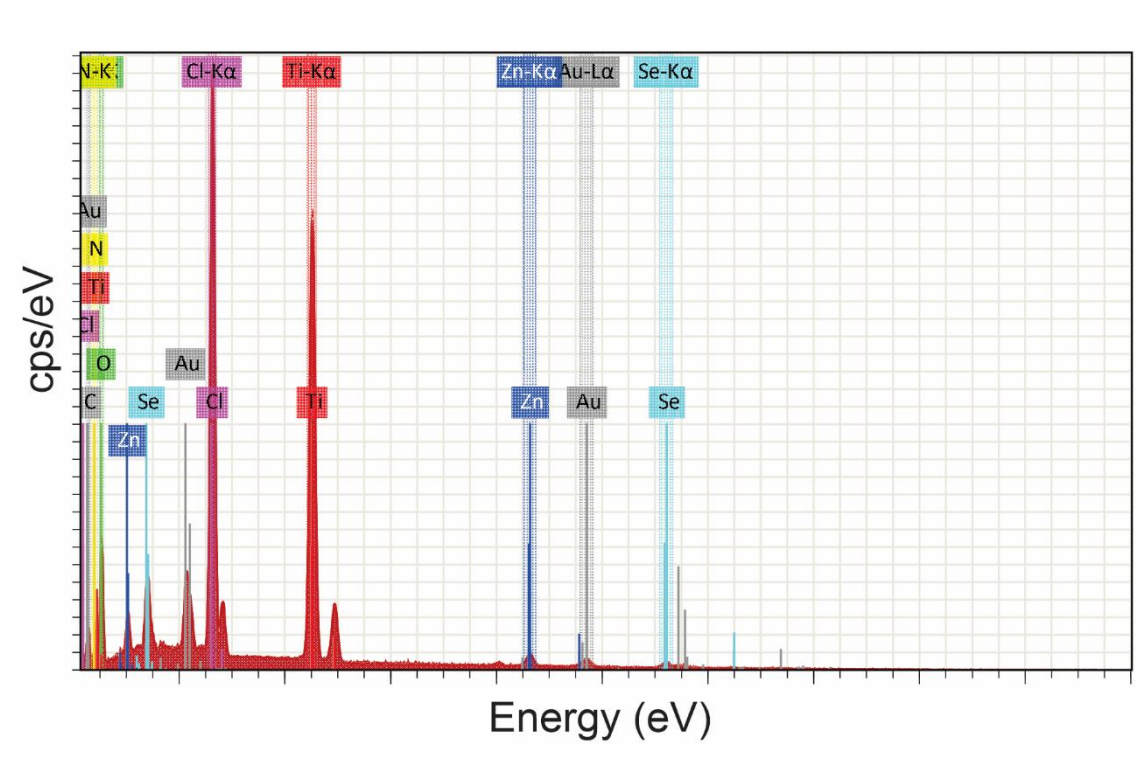

Figure S22. EDS spectrum for photocatalyst TiO_2-**1A**. The element Au comes from metallization process.

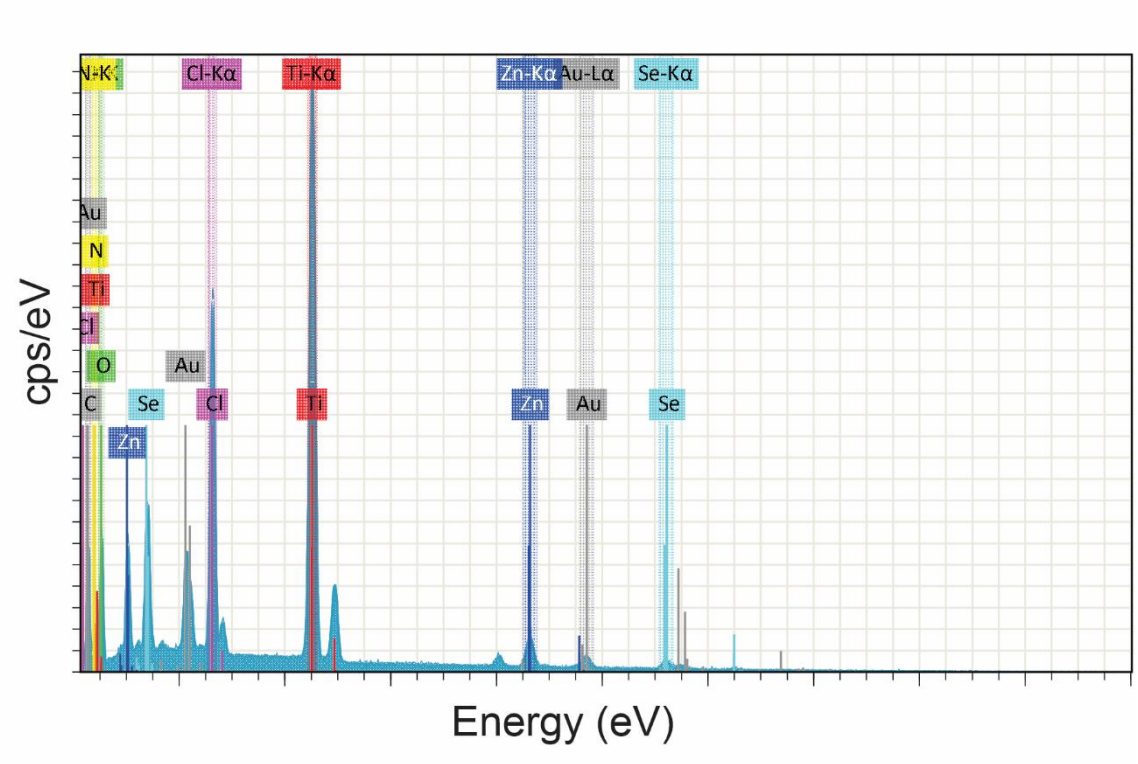

Figure S23. EDS spectrum for photocatalyst TiO_2-**2A**. The element Au comes from metallization process.

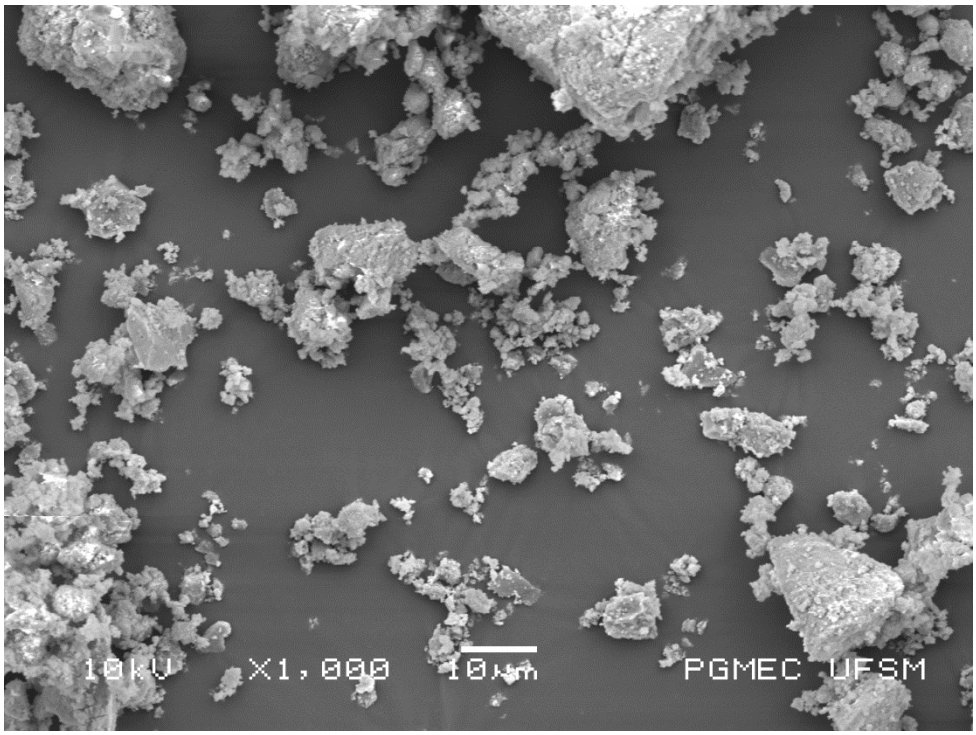

Figure S24. SEM images for photocatalyst TiO_2-**1A**.

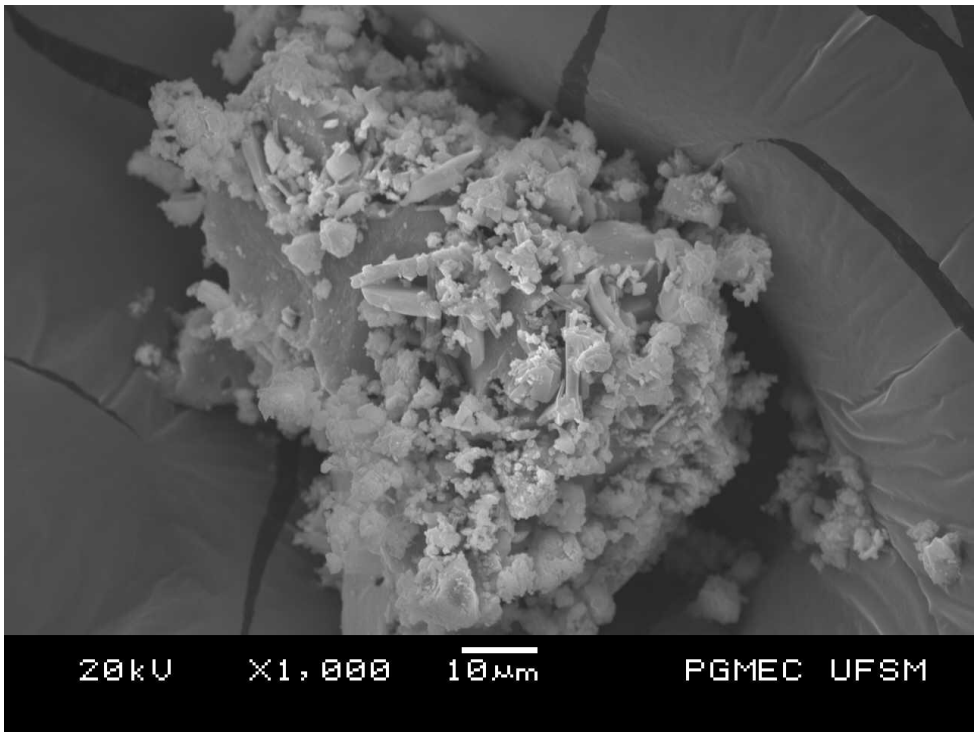

Figure S25. SEM images for photocatalyst TiO_2-**2A**.

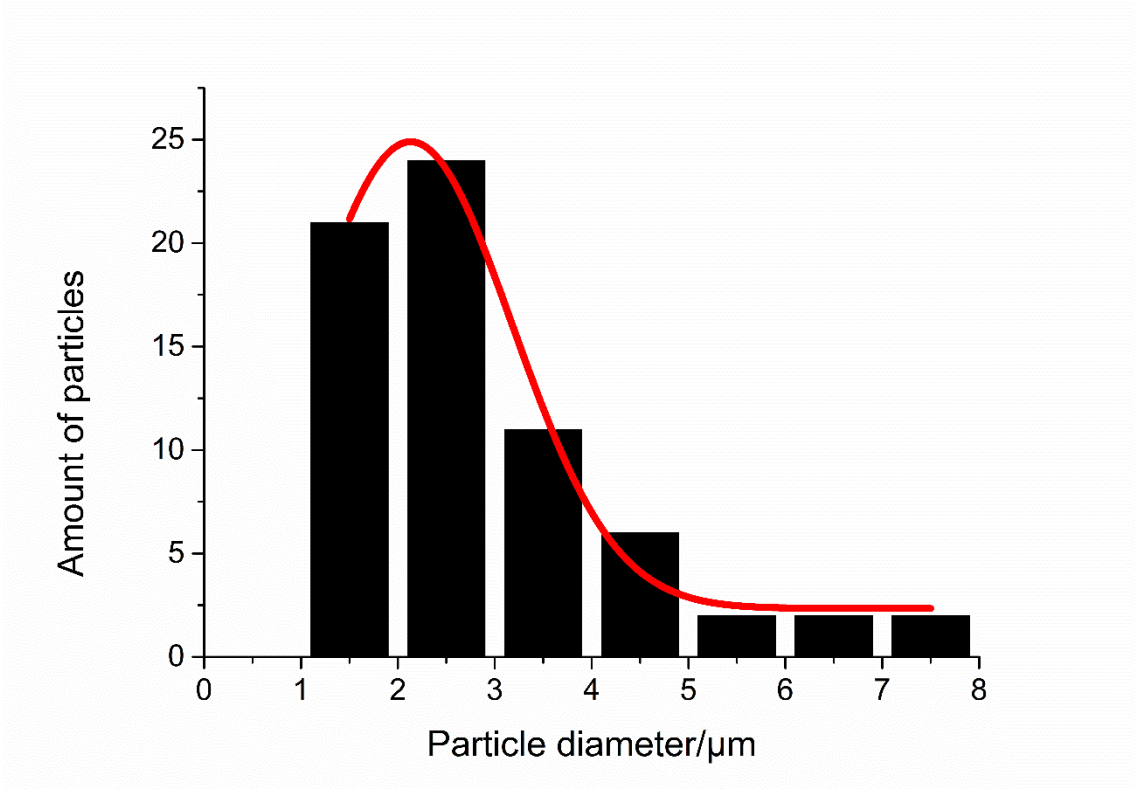

Figure S26. Particle size distribution for the photocatalyst TiO_2-**1A**.

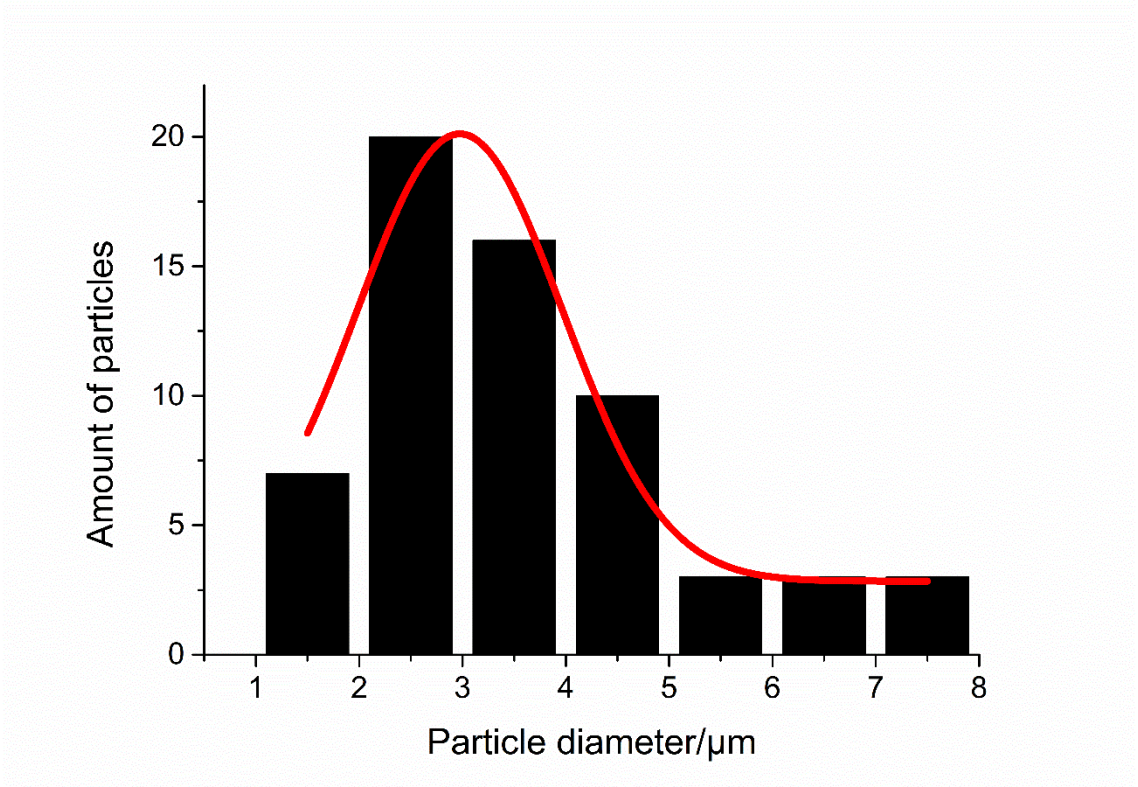

Figure S27. Particle size distribution for the photocatalyst TiO_2-**2A**.

Figure S28. Stainless steel reactor used in syntheses of compounds **1-3.**

Figure S29. System used in experiments applying photocatalyst TiO_2-**1A and** TiO_2-**2A** for hydrogen evaluation.

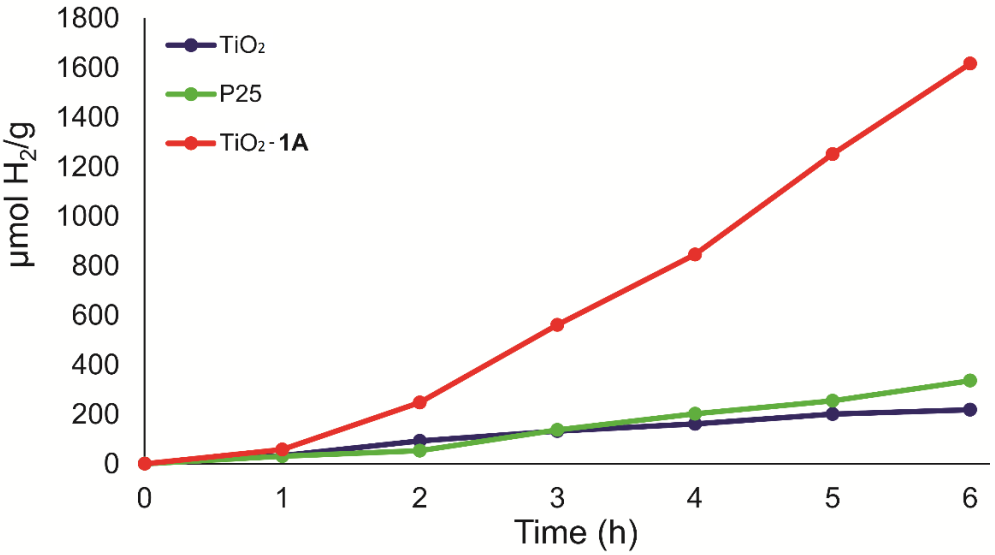

Figure S30. Photocatalytic activity of the photocatalyst TiO_2-**1A**.

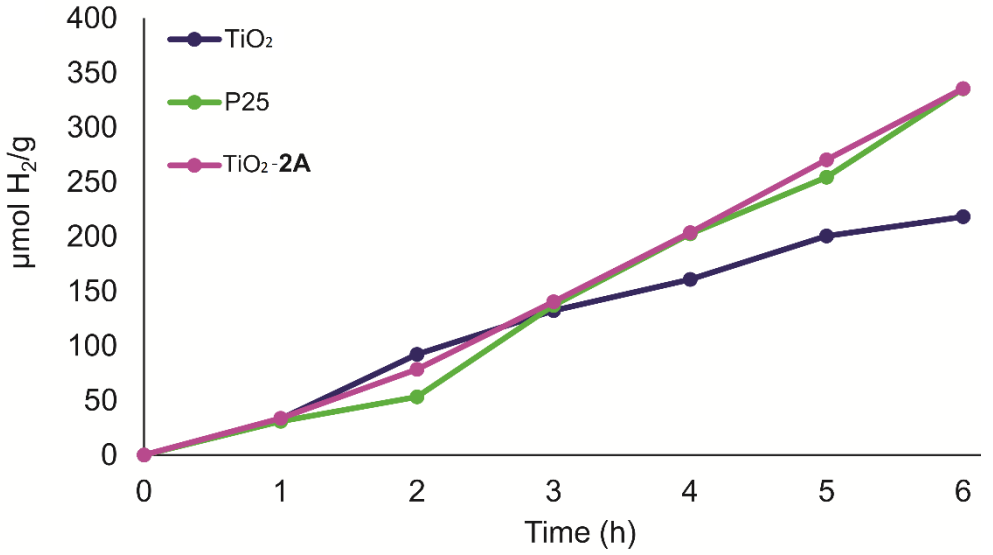

Figure S31. Photocatalytic activity of the photocatalyst TiO_2-**2A**.